J. Chem. Sci. Vol. 128, No. 6, June 2016, pp. 861–865. © Indian Academy of Sciences.
DOI 10.1007/s12039-016-1101-5

Catalytic activity of CuO-$Gd_{0.1}Ti_{0.1}Zr_{0.1}Ce_{0.7}O_2$ in CO oxidation

IGOR V ZAGAYNOV[a,*] and ELENA YU LIBERMAN[b]
[a]A A Baikov Institute of Metallurgy and Materials Science, Leninskii pr. 49, Moscow, Russia
[b]D Mendeleev University of Chemical Technology of Russia, Miusskaya sq. 9, Moscow, Russia
e-mail: igorscience@gmail.com

MS received 1 March 2016; revised 4 May 2016; accepted 5 May 2016

Abstract. (1-10wt.%) CuO-$Gd_{0.1}Ti_{0.1}Zr_{0.1}Ce_{0.7}O_2$ mesoporous catalysts were prepared by simple co-precipitation method with sonication and tested for CO oxidation. The catalysts show the highest activity due to better dispersion of CuO species as well as enhanced interaction between CuO and the developed support. It was shown that these systems have full conversion at temperature of 60–65°C.

Keywords. Ceria; copper oxide; CO oxidation.

1. Introduction

Carbon monoxide is a colorless and toxic gas. It can cause human beings to die in a short time.[1] CuO-CeO_2 catalysts have been shown to be very active for total oxidation of CO, exhibiting specific activities far superior to the conventional copper-based catalysts and comparable with or superior to platinum catalysts. Doped CeO_2-materials (solid solutions with a cubic crystal lattice) are considered as more promising systems for use in this goal as a support and is known as an oxygen buffer: it stores and releases oxygen when needed.[2,3] When combined with CuO, both metals show strong synergistic effects, especially in the copper loading in amount up to 10 mol%.[4] A synergistic effect between the ionic couples of Cu^+/Cu^{2+} and Ce^{3+}/Ce^{4+} results in higher interfacial redox activity, and the dispersion of copper is not a main factor.[5,6] The charge state of copper is also a key factor of the activity of catalysts, and it is known that the Cu^+ is the key active component for CO oxidation.[7] Many methods were proposed to synthesize CuO-CeO_2, because the properties of these materials are dependent on the initial properties of powder such as homogeneity, particle size, porous structure, phase purity, etc.[8–10] Therefore, in this work we describe the simplest synthesis of mesoporous nanoscale copper oxide-ceria solid solution catalysts by sonochemical method using inorganic salts without any additives (ultrasound irradiation can induce the formation of particles with much smaller size and higher surface area than those reported by other methods, and this technique has good reproducibility), and test in model CO oxidation reaction.

*For correspondence

2. Experimental

2.1 *Synthesis*

Cerium(III) nitrate, zirconyl nitrate, gadolinium nitrate, copper nitrate, and titanium(IV) chloride were used as metal precursors. Appropriate amounts of salts were dissolved in 500 mL distilled water containing of nitric acid (pH=2) to give final concentrations 0.04 M. Then, deposition was carried out by addition of 2.5 M KOH solution up to pH 10 at 30°C under stirring. Ultrasonic processing (10 min, 35 kHz, 150 W, Sapphire UZV-4.0) was used during dissolution of salts in distilled water and after precipitation. The resulting precipitates were filtered, washed with distilled water-ethanol solution (H_2O/C_2H_5OH=9 v/v), dried at 150°C for 12 h, and calcined in static air by heating at a rate of 4°C/min from room temperature to 500°C and kept at 500°C for 1 h in a muffle furnace. One calcined sample (5wt% CuO-$Gd_{0.1}Ti_{0.1}Zr_{0.1}Ce_{0.7}O_2$) was treated with nitric acid solution (pH 2, 30°C, 15 min. with sonication).

2.2 *Characterization*

Powder XRD data were collected at room temperature (DRON-3M, Russia) with CuK_α radiation. Particle size (d_{XRD}) measurements were made by applying the Scherrer equation to the full-width at half maximum after accounting for instrumental broadening using germanium as reference. Quantitative phase analysis was calculated by the Rietveld method.

Specific surface area (S_{BET}) of the powders was measured by a conventional (BET method) nitrogen sorption method at 77K (Tri Star 3000 Micromeritics).

Table 1. Main characteristics of synthesized samples.

No.	Sample	d_{XRD}, nm (support)	d_{XRD}, nm (CuO)	CuO phase (XRD), wt.%	CuO phase (EDS), wt.%	a(CeO_2), nm	S_{BET}, m^2g^{-1}	T_{100} (CO conversion), °C
0	$Gd_{0.1}Ti_{0.1}Zr_{0.1}Ce_{0.7}O_2$	9	–	–	–	0.5405	83	263
1	1wt.%CuO-$Gd_{0.1}Ti_{0.1}Zr_{0.1}Ce_{0.7}O_2$	9	–	–	*	0.5396	82	90
2	5wt.%CuO-$Gd_{0.1}Ti_{0.1}Zr_{0.1}Ce_{0.7}O_2$	6	–	–	4.7	0.5404	100	78
2a	5wt.%CuO-$Gd_{0.1}Ti_{0.1}Zr_{0.1}Ce_{0.7}O_2$	6	–	–	3.5	0.5395	87	70
3	10wt.%CuO-$Gd_{0.1}Ti_{0.1}Zr_{0.1}Ce_{0.7}O_2$	5	28	5	*	0.5397	80	82

2a – sample 2 was treated with nitric acid. * – not measured.

Pore-size distributions were calculated from desorption isotherm data using BJH method. Samples were degassed at 120°C for 5 h prior to measurement.

TEM analyses were conducted on an Omega Leo-912AB transmission electron microscope with accelerating voltage of 100 kV.

The elemental composition of the surface of catalysts (pressed pellets for better distribution for determination), for samples with 5wt% CuO was measured by energy-dispersive X-ray spectroscopy (EDS) based on a scanning electron microscope JEOL JSM 6510 LV with an X-ray microanalysis system INCA Energy 350 (Oxford Instruments).

The catalytic activity of the synthesized samples in the oxidation of CO was determined by the flow method at atmospheric pressure. The process was conducted in a U-shaped quartz reactor at a volumetric flow rate of 1800 h^{-1} within a temperature range of 20–100°C. The bulk volume of the precisely weighed portion of the catalyst powder loaded into the reactor was 1 cm^3. The temperature was measured with a thermocouple placed in the center of the catalytic bed. The model gas mixture had the following composition, vol%: CO – 4.2; O_2 – 9.6; N_2 – balance. The concentrations of CO, O_2 and N_2 were measured on Konik-Tech HRGC 5000B gas chromatograph.

3. Results and Discussion

XRD patterns of the catalysts are shown in figure 1. Samples 0-2a have one phase, consisting of ceria solid solution with a cubic fluorite structure (cF12) and only sample 3 with 10wt% CuO has additional monoclinic CuO phase (mC8). The result indicates (table 1) that

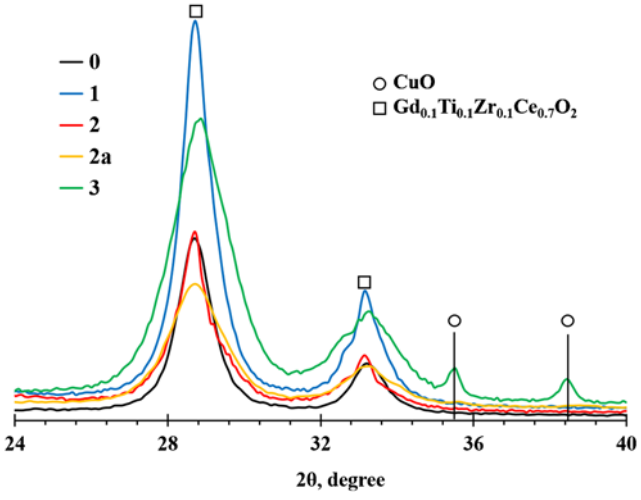

Figure 1. XRD patterns of powder samples with CuK_α radiation. See table 1 for composition of samples.

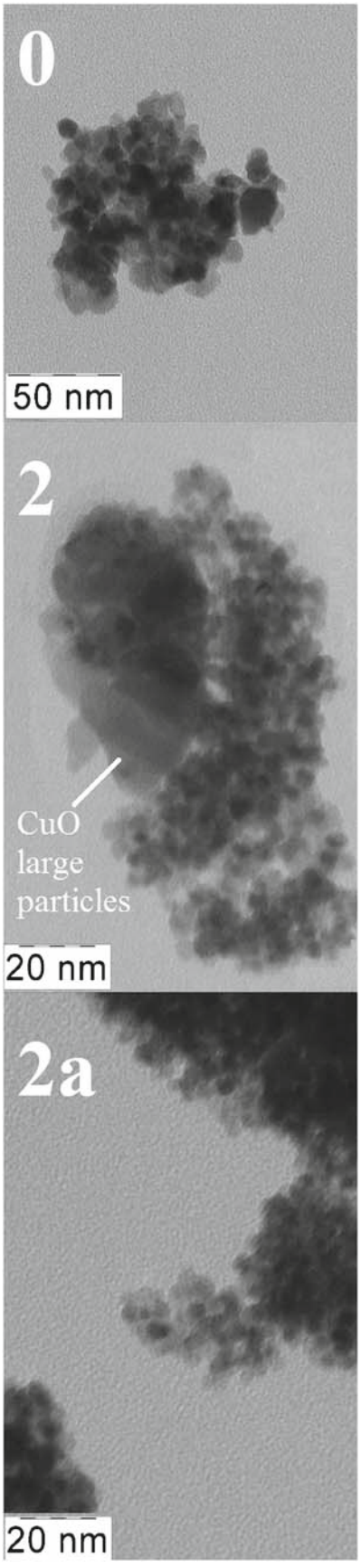

Figure 2. TEM microphotos of powder samples, calcined at 500°C.

the crystal size of the support becomes smaller as a result of the increase in copper content, which can be attributed to additional stabilization by Cu^{2+} in addition to Gd-Ti-Zr and/or to prevent large particles of individual CuO (figure 2). As can be seen in TEM, the individual particles are spherical: 6-15 nm – sample 0, 3-6 nm – samples 2, 2a, 3 (only about 20-30 nm of CuO particles in samples 2 and 3). The lattice parameter of ceria solid solution (a, table 1) has changed and indicate that some Cu^{2+} ions have been incorporated into the lattice to form Cu(Gd, Ti, Zr)–Ce–O solid solution, since Cu^{2+} ions are smaller than Ce^{4+} ions, and only sample 2 has similar parameter. These changes can be attributed to the coexistence of opposite effects: the substitution of larger Ce^{4+}(0.097 nm) by smaller Cu^{2+}(0.072 nm) contracts ceria cell; the formation of oxygen vacancies caused by the aliovalent doping (Ce^{4+} by Cu^{2+}) or creation of Ce^{3+}(0.103 nm) sites expands ceria cell; and also the coexistence of Cu^{2+}(0.072 nm) and Cu^{+} (0.077 nm) ions in these systems,[11,12] because some

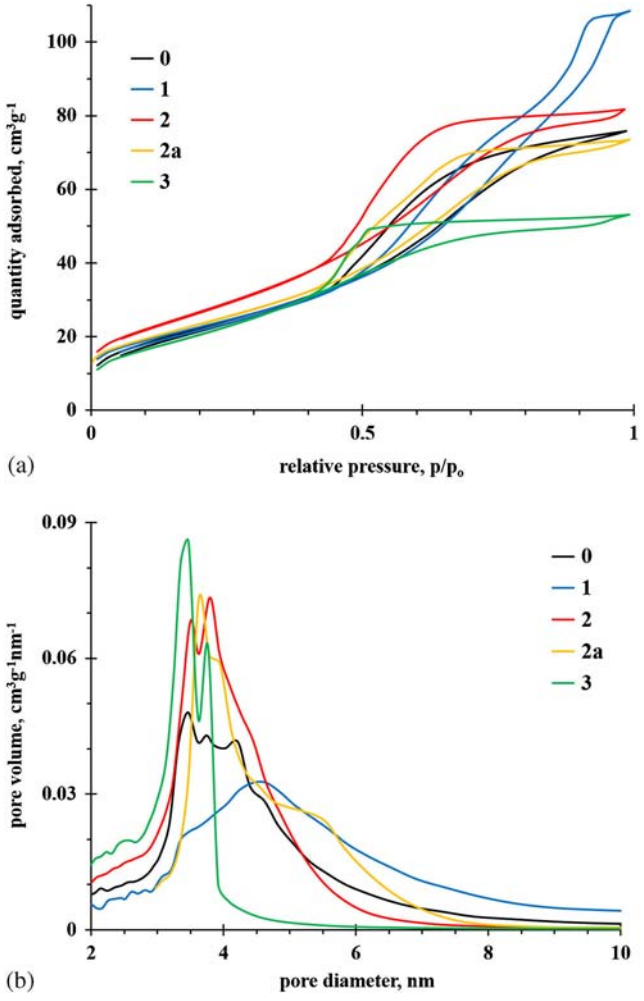

Figure 3. (a) Adsorption-desorption isotherms and; (b) pore size distributions.

part of CuO can be diluted in ceria solid solution in accordance with XRD (but small CuO particles up to 2-3 nm cannot be detected by XRD). This assumption can be confirmed by EDS investigation of the surface (table 1). It is shown that after acid treatment the quantity of copper was decreased, and Cu can be present either as small CuO particles or diluted in the ceria lattice. Therefore, it can be concluded that the samples have the following Cu species: large CuO particles (20-30 nm), small CuO particles (up to 10 nm), and Cu in the ceria lattice (in state 2+ and 1+), and only small CuO particles and Cu-containing solid solution in sample 2a.

Samples exhibit IV type adsorption curves with a hysteresis loop, indicating the presence of mesopores in the systems (figure 3a). The hysteresis loops correspond to the type of H2, i.e., the presence of different pore shapes (individual and/or associated cylindrical and/or bottle pores). Pores have size of 2-8 nm (figure 3b). The specific surface of the powders initially increases with the increase of CuO content, that may be associated with additional contribution of CuO surface (sample 2a has the same surface as sample 0), and then decreases due to the blocking of the support pores by Cu species, which is confirmed by pore size distribution (figure 3b, pore becomes narrower from sample 0 to sample 3).

Figure 4 shows CO oxidation activity of the catalysts. Sample 0 has no activity at temperature of 20–100°C,[13]

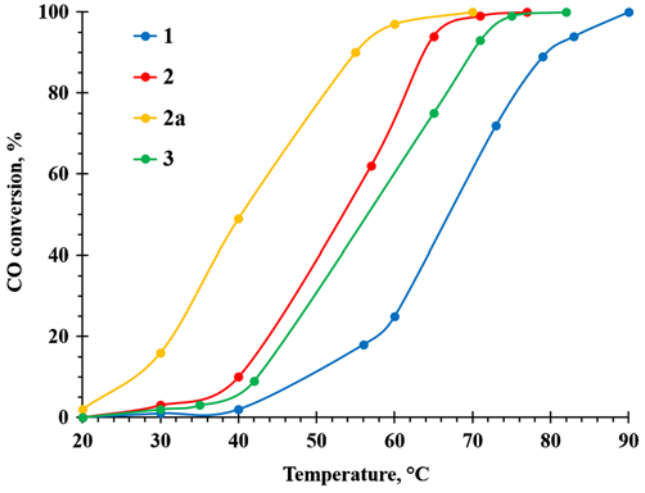

Figure 4. Temperature dependence of the conversion of carbon monoxide.

and the most significant synergetic effect between copper oxide-ceria occurs with addition of copper oxide in amount of 5-10 wt%, which is clearly seen in table 1. So, the most active catalyst is sample 2 (in the series of samples 1, 2 and 3). Moreover, by using nitric acid treatment, the contribution of Cu species to CO oxidation can be distinguished. The sample 2a is the most effective catalyst, and the activity is guaranteed by solid solution $Cu_xGd_{0.1}Ti_{0.1}Zr_{0.1}Ce_{0.7-x}O_2$ and very finely dispersed species of CuO (large CuO particles are active at higher reaction temperature) and has higher activity than reported in the previous work[12] at almost the same experimental conditions. This corresponds to literature data on the high activity for CO oxidation over copper-promoted ceria compared to unpromoted[5,14] ceria but in the previous work[15] it was demonstrated that after a nitric acid treatment the temperature of the catalyst for full conversion of CO was increased by more than 100°C, that authors associated with only the role of Cu^+ in CuO dispersed nanoparticles on a support (it is more pronounced than that of Cu-Ce-O solid solution).

Based on our and other mentioned works, we can propose the possible mechanism (figure 5) and conclude that the reaction takes place at the interface. CO is covered with strongly bound CO and the process is controlled by the interaction of adsorbed CO and O_2; also, since ceria-based material is a reducible support, participation of its lattice oxygen in the reaction must be concerned. The copper-doped ceria can produce high density of oxygen vacancies, physisorbed and chemisorbed sites for carbon monoxide. The active copper ions remain as Cu^+ during the catalytic cycle (the fraction of the intermediate carbonyl–Cu^{2+} is very low, and the fraction of carbonyl-Cu^+ species is much greater than Cu^+ and carbonyl–Cu^{2+})[16] and oxygen is directly provided by ceria lattice for carbon dioxide production (Mars van-Krevelen model). Adsorbed O_2 reacts with catalyst surface and forms highly reactive O_2^- anion at the oxygen vacancy site, and chemisorbed CO reacts with O_2^- to generate carbon dioxide and leave oxygen vacancy, then, oxygen vacancy is replenished by the gas-phase oxygen (Langmuir-Hinshelwood model).[17–20]

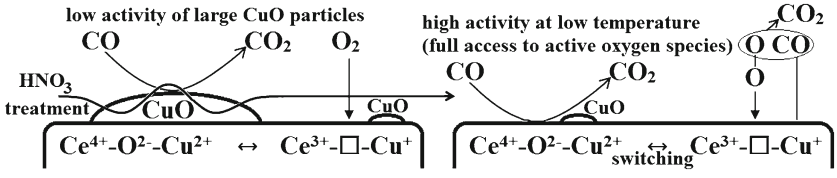

Figure 5. Schematic illustration of the possible mechanism of CO oxidation (□ - oxygen vacancy).

4. Conclusions

This work demonstrates the relationship between the structure and catalytic behavior for CO oxidation over CuO-$Gd_{0.1}Ti_{0.1}Zr_{0.1}Ce_{0.7}O_2$. The catalysts, prepared by the simple co-precipitation method, contain surface CuO, large (20-30 nm) and small (up to 10 nm) particles and Cu in a support lattice, forming a solid solution. The surface CuO species (large particles) can be removed by a nitric acid treatment. The catalyst shows the highest activity due to better dispersion of CuO species as well as enhanced interaction between CuO and the support. This strong interaction can induce the formation of large amount of oxygen vacancies and activate the lattice oxygen, which is beneficial to the higher activity for CO oxidation. The presence of Cu^{+}/Cu^{2+}, Ce^{3+}/Ce^{4+}, oxygen vacancy/O^{2-}, and mesoporous nature of catalyst result in high activity of CO oxidation. Furthermore, the detailed mechanism of CO oxidation over copper oxide promoted catalysts need to be investigated, especially the ratio of Langmuir-Hinshelwood and Mars van-Krevelen models in this reaction.

References

1. Royer S and Duprez D 2011 *ChemCatChem* **3** 24
2. Venkataswamy P, Jampaiah D, Aniz C U and Reddy B M 2015 *J. Chem. Sci.* **127** 1347
3. Vinodkumar T, Durgasri D N, Maloth S and Reddy B M 2015 *J. Chem. Sci.* **127** 1145
4. Qi L, Yu Q, Dai Y, Tang C, Liu L, Zhang H, Gao F, Dong L and Chen Y 2012 *Appl. Catal. B* **119–120** 308
5. Liu W and Flytzani-Stephanopoulos M 1995 *J. Catal.* **153** 304
6. Luo M-F, Ma J-M, Lu J-Q, Song Y-P and Wang Y-J 2007 *J. Catal.* **246** 52
7. Tang X, Zhang B, Li Y, Xu Y, Xin Q and Shen W 2004 *Catal. Today* **93-95** 191
8. Snytnikov P V, Stadnichenko A I, Semin G L, Belyaev V D, Boronin A I and Sobyanin V A 2007 *Kinet. Catal.* **48** 439
9. Snytnikov P V, Stadnichenko A I, Semin G L, Belyaev V D, Boronin A I and Sobyanin V A 2007 *Kinet. Catal.* **48** 448
10. Zagaynov I V 2015 *Mater. Res. Bull.* **61** 36
11. Fu G-Y, Mao D-S, Sun S-S, Yu J and Yang Z-Q 2015 *J. Ind. Eng. Chem.* **31** 283
12. Zheng Y, Mao D, Sun S and Fu G 2015 *J. Nanopart. Res.* **17** 471
13. Zagaynov I V, Liberman E Yu and Naumkin A V 2015 *Surf. Sci.* **642** L11
14. Galvita V, Filez M, Poelman H, Bliznuk V and Marin G M 2014 *Catal. Lett.* **144** 32
15. Jia A-P, Hu G-S, Meng L, Xie Y-L, Lu J-Q and Luo M-F 2012 *J. Catal.* **289** 199
16. Moreno M, Bergamini L, Baronetti G T, Laborde M A and Marino F J 2010 *Int. J. Hydrogen Energ.* **35** 5918
17. Lu J Q, Sun C X, Li N, Jia A P and Luo M F 2013 *Appl. Surf. Sci.* **287** 124
18. Martínez-Arias A, Fernández-García M, Gálvez O, Coronado J M, Anderson J A, Conesa J C, Soria J and Munuera G 2000 *J. Catal.* **195** 207
19. Jia A P, Jiang S Y, Lu J Q and Luo M F 2010 *J. Phys. Chem. C* **114** 21605
20. Li Y, Cai Y, Xing X, Chen N, Deng D and Wang Y 2015 *Anal. Methods* **7** 3238